Organic Electronics 13 (2012) 939–944

Contents lists available at SciVerse ScienceDirect

Organic Electronics

journal homepage: www.elsevier.com/locate/orgel

High current conduction with high mobility by non-radiative charge recombination interfaces in organic semiconductor devices

Woo Sik Jeon, Jung Soo Park, Ling Li, Dae Chul Lim, Young Hoon Son, Min Chul Suh *, Jang Hyuk Kwon *

Department of Information Display, Kyung Hee University, Dongdaemoon-gu, Seoul 130-701, Republic of Korea

ARTICLE INFO

Article history:
Received 27 June 2011
Received in revised form 26 January 2012
Accepted 17 February 2012
Available online 2 March 2012

Keywords:
Charge generation
Recombination
p-n Junction
Low voltage

ABSTRACT

We report a unique non-radiative p-n-p junction structure to provide high current conduction with high mobility in organic semiconductor devices. The current conduction was improved by increasing p-n junctions made with intrinsic p-type hole transport layer and n-type electron transport layer. The excellent hole mobility of 5.3×10^{-1} $cm^2/V\,s$ in this p-n-p device configuration is measured by the space charge limited current method with an electric field of 0.3 MV/cm. Enhanced current conduction of 248% at 4.0 V was observed in fluorescent blue organic light-emitting diodes with introduction of non-radiative p-n-p-n-p junction interfaces. Thereupon, the power efficiency at 1000 cd/m^2 was improved by 22% and the driving voltage also was reduced by 17%, compared to that of no interface device. Such high current conduction with high mobility is attributed to the carrier recombination at p-n-p interfaces through coulombic interaction. This non-radiative p-n-p junction structure suggested in this report can be very useful for many practical organic semiconductor device applications.

Crown Copyright © 2012 Published by Elsevier B.V. All rights reserved.

1. Introduction

The reduction of operating voltage and the realization of high carrier mobility in organic semiconductor devices such as organic light-emitting diode (OLED) and organic transistor is the most important issue because it is directly correlated to the power consumption and rapid switching performances of the devices. Generally, operating voltage and carrier mobility of organic semiconductor devices is greatly affected by charge injection situation and carrier transporting characteristics. Therefore, the use of materials with high carrier mobility as well as a good ohmic contact property at the metal interface is the most desirable approach for the high performance devices. However, finding such materials normally demands considerable investment of time and effort. Hence as an alternative approach, the efficient interface materials such as a thin insulator and a strong dipole layer at the electrode have been reported [1–6]. In particular, the organic materials with low LUMO (lowest occupied molecular orbital) values and inorganic buffer materials with low conduction band on the electrode were well known as good hole injection layers [3–8]. Such a good injection may be attributed to the generation of the strong interface dipoles and/or new energy states between organic and metal interfaces, which results in significant injection barrier reduction [6,9]. The main reason for such efficient carrier injection in these configurations is their good energy level alignment between Fermi level of metal electrode and organic layer [6,10,11].

To obtain intrinsically high mobility from the organic materials, many research groups have investigated to make high crystalline phase molecular films with various deposition techniques [12–18]. This approach can provide easy carrier hopping in organic films [19].

In this investigation, we report a new methodology to realize a high current conduction in organic semiconductor devices based on the Langevin recombination theory [20]. Langevin suggested that current density (J) attracted by coulombic interaction between holes and electrons within Langevin radius could be expressed by following equation:

* Corresponding authors. Tel.: +82 2 961 0948; fax: +82 2 961 9154.
E-mail addresses: mcsuh@khu.ac.kr (M.C. Suh), jhkwon@khu.ac.kr (J.H. Kwon).

1566-1199/$ - see front matter Crown Copyright © 2012 Published by Elsevier B.V. All rights reserved.
doi:10.1016/j.orgel.2012.02.008

$$J = n_h e \mu_t F$$

where e is the unit charge, n_h is hole densities, F is the electric field, and μ_t ($\mu_t = \mu_e + \mu_h$) is total mobility. μ_e and μ_h are the electron and hole mobility, respectively. In general, hole or electron conduction in p- or n-type organic semiconductor materials uses only hole mobility or electron mobility. However, in this equation we expect that both mobilities of hole and electron can contribute to make the current conduction in organic semiconductor devices. If recombination interface is generated by p-n junctions in organic semiconductor devices, we may generate enhanced current conduction from both contributions of hole and electron mobilities within Langevin radius. Langevin gave an expression for the coulombic capture radius,

$$r_c = e^2/(4\pi\varepsilon_r\varepsilon_0 k_B T)$$

where ε_0 is the vacuum permeability, ε_r is the relative dielectric constant of the semiconductor, T is the temperature, and k_B is the Boltzmann's constant, respectively. This relation is valid if we suppose a much smaller mean-free path compared to the thermal capture radius because charge transport normally takes place by hopping between molecules and the mean-free path is on the order of the intersite distance (a) of ≈1–2 nm. At room temperature and with a relative dielectric constant (ε_r) of ≈3, typical for organic semiconductors, the thermal capture radius (r_c) is ≈18.5 nm.

In order to see such kinds of current conductions, multiple p-n junction layers were formed by stacking of electron transporting layer with low-lying LUMO and hole transporting layer with high-lying HOMO (highest occupied molecular orbital) as shown in Fig. 1(a). Charge generation interfaces with chare recombination interfaces can be generated by these multiple p- and n- junctions. Enhanced current conduction and high mobility by this chare recombination interface of multiple p-n junctions are reported.

2. Experimental section

The sublimated grade *N*,*N*′-bis(naphthalen-1-yl)-*N*,*N*′-bis(phenyl)benzidine (NPB), *N*,*N*′-di[4-(*N*,*N*′-diphenylamino)phenyl]-*N*,*N*′-diphenylbenzidine (DNTPD), and 4,4′,4″-tris(*N*-(2-naphthyl)-*N*-phenyl-amino)triphenylamine (2-TNATA) as intrinsic p-type materials and 1,4,5,8,9,11-hexaazatriphenylene-hexacarbonitrile (HATCN) as an intrinsic n-type material were purchased by Lumtec Corp. and used without purification, respectively. The molecular structure of HATCN, DNTPD, and 2-TNATA are shown in Fig. 1(b). Sublimated grade 2-methyl-9,10-di(2-naphthyl)anthracene (MADN), *p*-bis(*p*-*N*,*N*-diphenyl-aminostyryl)benzene (BD-1), lithium quinolate (Liq), and 1,3,5-tris(m-pyrid-3-ylphenyl)benzene (TmPyPB) were used for the device fabrication of blue OLEDs. To fabricate hole and electron only devices and blue OLEDs, glass substrates pre-coated with a 150 nm thick indium tin oxide (ITO) film with a sheet resistance of ~10 Ω/square were used. The line patterns of the ITO layer and insulator covering for active area were formed by photolithography. Before any other material deposition, the patterned ITO glass was cleaned by sonification in an isopropylalcohol and rinsed in deionized water, and finally irradiated in a UV-ozone chamber. All organic layers and MoO_3 were deposited in a multi-chamber vacuum system at a base pressure of 10^{-7} Torr. Al (100 nm) was deposited in an adjacent metal chamber. The deposition rate for all organic layers and MoO_3 was about 0.5 Å/s and 0.1 Å/s, respectively. Then an Al electrode was deposited at 5 Å/s. Thickness of each organic and inorganic layer was controlled by the effusion rates using a quartz-crystal microbalance (Cygnus™ of Inficon Co.). The active area of the fabricated devices was 2×2 mm^2. To prevent the influence of the ambient oxygen, all devices were encapsulated with glass and epoxy sealant in a N_2 atmosphere glove box. The current density–voltage (*J*–*V*) of blue OLEDs was measured using a Keithley SMU 2635A and their luminance–voltage (*L*–*V*) with a Minolta CS-100A. The electroluminescence (EL) spectra and CIE color parameters were obtained with a Minolta CS-1000A spectroradiometer. The current–voltage (*J*–*V*) characteristics for hole only devices were carried out using an Agilent 4156C semi-conductor parameter analyzer.

3. Results and discussion

NPB has a HOMO value of ~5.4 eV while HATCN has a LUMO value of ~5.7 eV [21] as shown in Fig. 1(a). Intrinsically NBP and HATCN are p-type material and n-type material, respectively, because their HOMO and LUMO levels are close to Fermi level of general electrode metals. The energy offset between HOMO of NPB and LUMO of HATCN is 0.3 eV when we consider intrinsic energy levels of these two materials. However, the real energy offset at the interface between NPB and HATCN is totally reverse according to the recent report by Kim et al. (LUMO of HATCN lies over 0.3 eV level than HOMO of NPB) [6]. Anyhow, this barrier is small enough to be easily overcome at room temperature. When we make a p-n junction interface with these p- and n- materials, charge generation behavior can be generated because it separates hole and electrons at the junction. Substantially, there have been several reports that demonstrated a good charge generation behavior [6,10,11]. When we stacked p-n-p multiple interfaces, hole current can flow without any serious barrier as shown in Fig. 1(a). In this device configuration, one interface (right side of HATCN layer) can work as a charge generation part and the other interface (left side of HATCN layer) can work as a charge recombination part. In order to investigate improved current conduction by charge recombination effect, three different types of hole only devices were fabricated as follows:

Device A: ITO/HAT-CN (40 nm)/NPB (60 nm)/MoO_3 (5 nm)/Al;
Device B: ITO/MoO_3 (0.75 nm)/NPB (30 nm)/HAT-CN (40 nm)/NPB (30 nm)/MoO_3 (5 nm)/Al;
Device C: ITO/MoO_3 (0.75 nm)/NPB (20 nm)/HAT-CN (20 nm)/NPB (20 nm)/HAT-CN (20 nm)/NPB (20 nm)/MoO_3 (5 nm)/Al.

Here, MoO_3 was used to make ohmic contact between ITO and NPB as well as electron injection barrier from Al

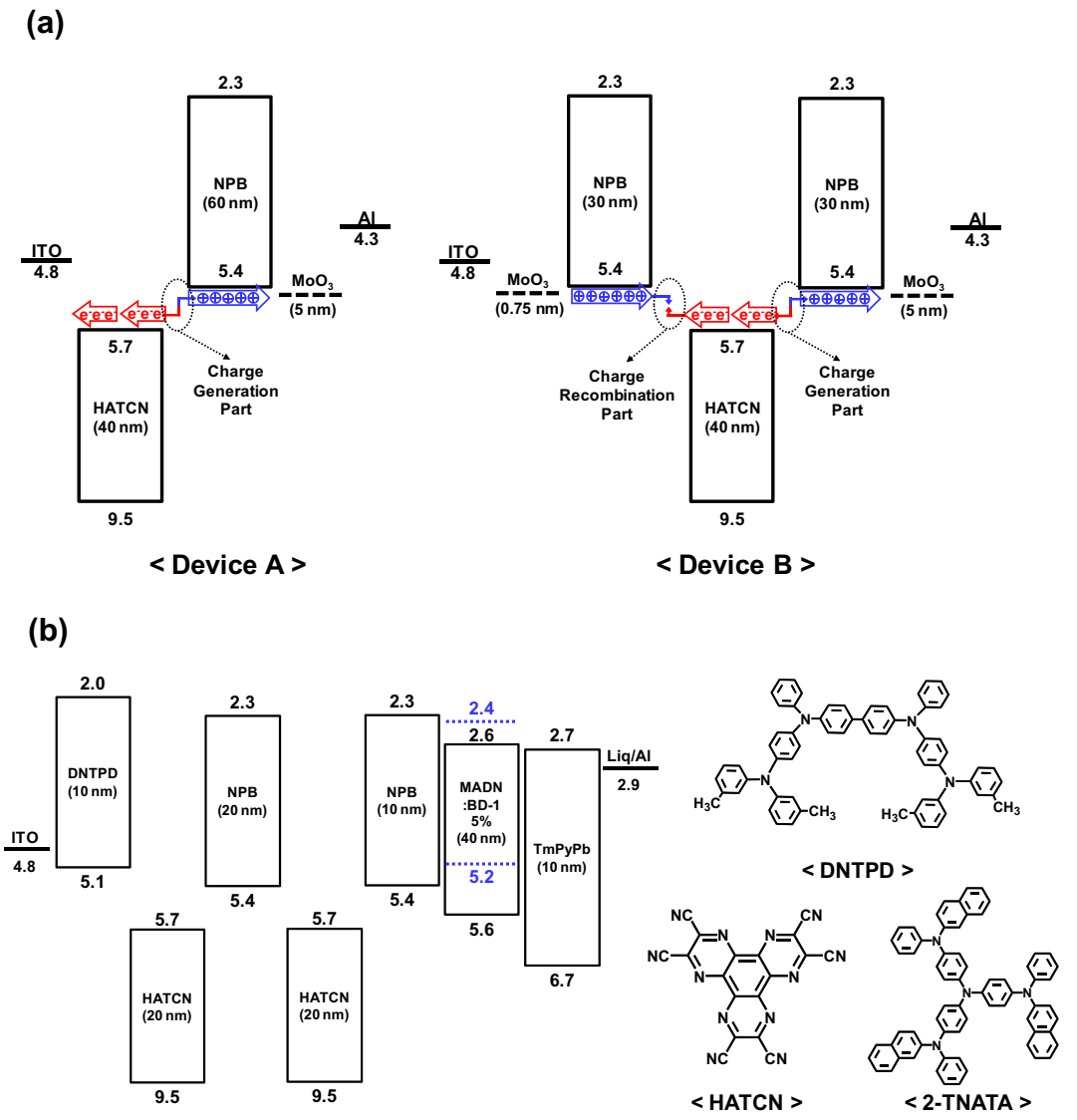

Fig. 1. (a) Device structure of hole-only devices, (device A and B) (b) devices structure of blue fluorescent OLEDs with p-n-p-n junction interface.

to NPB. As shown in Fig. 1(a), the Device A has one charge generation interface while Device B and C are able to form charge generation as well as recombination interfaces as p-n-p structures. We used the same thickness of HATCN layer in all devices to investigate only chare recombination effects. Fig. 2 shows the current density (J) versus voltage (V) characteristics which is originated from the hole current flows of those devices (Devices A ~ C). At a given constant voltage of 1.0 V, the current densities are 5.03 mA/cm^2, 12.92 mA/cm^2, and 41.76 mA/cm^2 for Device A, B, and C, respectively. A lowest current flow was observed for the Device A. When the p-n-p and p-n-p-n-p junctions were employed in the hole only devices, hole current conduction was dramatically improved by 257% and 830% compared with Device A at 1 V.

In order to understand effectiveness more by charge recombination interfaces, measurements of carrier

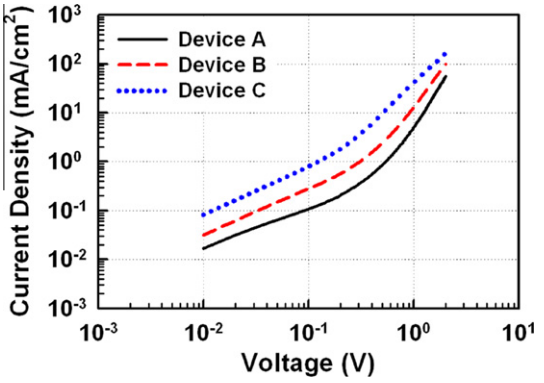

Fig. 2. Current density vs. voltage characteristics of hole-only devices A ~ C.

mobility of each material as well as the HTL(hole transport layer)/HATCN/HTL stack are very interesting. Fortunately, these p-n-p stacked devices show very good SCLC (space charge limited current) behaviors as shown Fig. 3(a). The measurement of carrier mobility by the SCLC method was applied to our devices [22]. For the evaluation of carrier mobility in single and p-n-p stacked devices, we fabricated the following hole and electron only devices:

Device D: ITO/MoO_3 (0.75 nm)/α-NPB (100 nm)/MoO_3 (5 nm)/Al;
Device E: ITO/MoO_3 (0.75 nm)/2-TNATA (100 nm)/MoO_3 (5 nm)/Al;
Device F: ITO/HATCN/Al;
Device G: ITO/MoO_3 (0.75 nm)/α-NPB (20 nm)/HAT-CN (60 nm)/α-NPB (20 nm)/MoO_3 (5 nm)/Al;
Device H: ITO/MoO_3 (0.75 nm)/2-TNATA (20 nm)/HAT-CN (60 nm)/2-TNATA (20 nm)/MoO_3 (5 nm)/Al.

The low mobility 2-TNATA (2×10^{-5} cm^2/Vs) [23] and well known high mobility NPB materials (3×10^{-4} cm^2/Vs) [23] was evaluated as a hole only device to prove the effectiveness of carrier mobility enhancement. An electron only device (Device F) also was evaluated to see the effectiveness of carrier mobility enhancement. The carrier mobility to electric field dependence, μ (E), in our devices

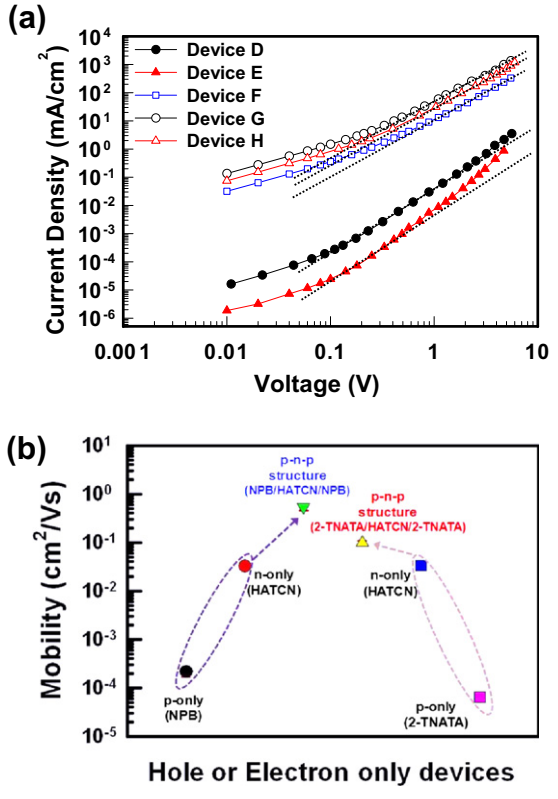

Fig. 3. (a) current density–voltage characteristics of device D ~ H. (Dotted lines mean ideal SCLC curves) (b) Mobility characteristics of p-only, n-only, and p-n-p devices.

was plotted using the reported method [22]. The measured mobilities were as follows: $2.2 \pm (0.2) \times 10^{-4}$ cm^2/Vs (hole mobility) for NPB (Device D), $6.4 \pm (0.3) \times 10^{-5}$ cm^2/Vs (hole mobility) for 2-TNATA (Device E), and $3.3 \pm (0.1) \times 10^{-2}$ cm^2/Vs (electron mobility) for HAT-CN (Device F) at 0.3 MV/cm, respectively. The mobilities of NPB and 2-TNATA are consistent with those reported in previous paper [23]. Devices G and H gave $5.3 \pm (0.3) \times 10^{-1}$ cm^2/Vs and $9.9(\pm 0.4) \times 10^{-2}$ cm^2/Vs of hole mobilities at the 0.3 MV/cm of electric field, respectively (see Fig. 3(b)). By insertion of the HATCN layer between HTLs, the hole carrier mobility was remarkably increased for more than one order of magnitude. The increased mobility values of Devices G and H is much higher than intrinsic electron mobility of HATCN, indicating current conduction by both contributions of hole and electron mobility are existed within Langevin coulombic capture radius.

To precisely investigate the effect of real devices, blue fluorescent OLEDs with various hole transport systems were fabricated. The device structures and the materials used for this study are shown in Fig. 1(b). The MADN as a fluorescent host, BD-1 as a fluorescent dopant, Liq as a electron injection layer, and TmPyPB as a electron transporting layer were used for device fabrication [24]. The detailed device structures with those blue fluorescent materials were as follows:

Device I: ITO/HATCN (40 nm)/NPB (40 nm)/MADN: BD-1 (5%, 40 nm)/TmPyPb (10 nm)/Liq (1 nm)/Al (100 nm);
Device J: ITO/DNTPD (20 nm)/HATCN (40 nm)/NPB (20 nm)/MADN: BD-1 (5%, 40 nm)/TmPyPb (10 nm)/Liq (1 nm)/Al (100 nm);
Device K: ITO/DNTPD (10 nm)/HATCN (20 nm)/NPB (20 nm)/HATCN (20 nm)/NPB (10 nm)/MADN: BD-1 (5%, 40 nm)/TmPyPb (10 nm)/Liq (1 nm)/Al (100 nm).

The Device I was designed as a control device, which has no charge recombination interface. The Devices J and K were designed to investigate p-n-p junction effects. Here, DNTPD as a hole injection layer was used to minimize the hole injection barrier at the ITO interface. DNTPD has a HOMO level of 5.1 eV. The doping concentration in the EML was fixed by 5% in all the devices. Fig. 4(a) shows the *J–V–L* and efficiency characteristics of the Devices I ~ K. The turn-on (at 1 cd/m^2) and operating voltages (at 1000 cd/m^2) of 2.7 V and 5.2 V are obtained in the Device I. Operating voltage is decreased to 4.3 V in Device K with increasing p-n-p junctions. Conversely, current density is increased from 6.46 mA/cm^2 to 16.07 mA/cm^2 at 4.0 V. Enhanced current conduction of 248% at 4.0 V was observed in fluorescent blue organic light-emitting diodes with introduction of non-radiative p-n-p-n-p junction interfaces. Especially, driving voltages and current density improvement at the multiple p-n-p junction device were noticed. This result indicates that charge recombination interfaces are very effective in reducing driving voltage with increasing current conduction.

Fig. 4(b) shows power efficiencies as a function of luminance. The power efficiency at 1000 cd/m^2 was 2.98 lm/W in the Device K (four p-n junction), which is ~21.6% improved result compared to that of Device I (2.45 lm/W).

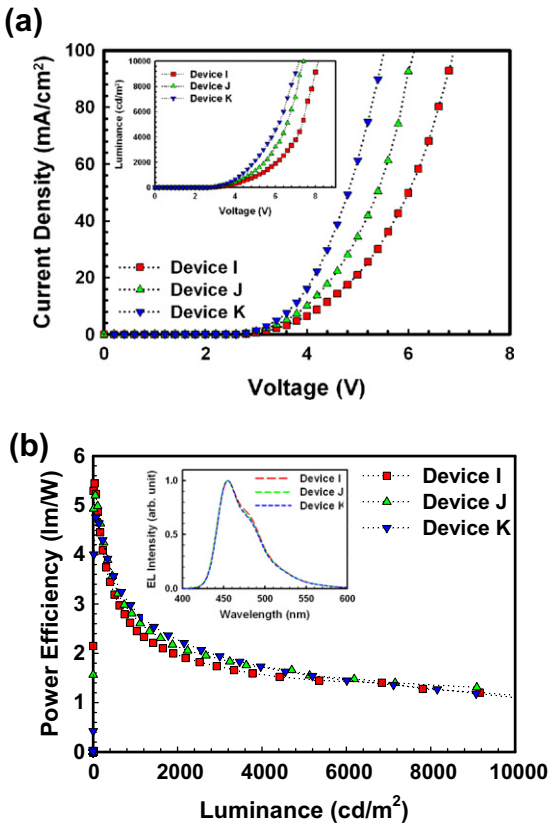

Fig. 4. (a) Current density vs. voltage characteristics of blue fluorescent devices I ~ K, (Inset) luminance vs. voltage characteristics of blue fluorescent devices I ~ K. (b) Power efficiency as a function of luminance of the devices I ~ K. (Inset) Electroluminance spectra of devices I ~ K at 1000 cd/m^2 brightness.

The performances of all the devices are summarized in the Table 1. Although much improved *J–V–L* characteristics are obtained in the Device K, efficiency improvement under 1000 cd/m^2 is not so effective. We did not optimize for charge balance at the low current level. Therefore, some unbalanced charges may contribute power efficiency value under 1000 cd/m^2 brightness value. A constant peak maxima at 455 nm was observed in the EL spectrum of the Devices I ~ K at 1000 cd/m^2 brightness value shown in the inset of Fig. 4(b), which means that the recombination zone is not moved seriously even after introducing the multi-junction interfaces.

Indeed, we observed interesting and unique results associated with very low driving voltages and high power efficiency characteristics of hole only devices as well as fluorescent blue devices. These results could be explained by simultaneous charge generation and recombination process at p-n junction interfaces. In a charge generation interface, the slight increase of driving voltage is inevitable due to a Fermi level mismatching. In our charge generation interface, Fermi level mismatching is almost negligible according to the previous UPS study [6]. In addition, charge recombination interfaces could decrease a resistance for carrier transportation as suggested by Langevin

Table 1
Performances of fluorescent blue devices I ~ K.

	Device I	Device J	Device K
Turn-on voltage (1 cd/m^2)	2.7 V	2.7 V	2.7 V
Operating voltage (1000 cd/m^2)	5.2 V	4.7 V	4.3 V
Efficiency (1000 cd/m^2)	4.05 cd/A 2.45 lm/W	4.10 cd/A 2.80 lm/W	3.98 cd/A 2.98 lm/W
Efficiency (maximum)	5.32 cd/A 5.44 lm/W	5.07 cd/A 5.20 lm/W	4.72 cd/A 4.75 lm/W
CIE (x, y) (1000 cd/m^2)	(0.144, 0.132)	(0.144, 0.132)	(0.144, 0.131)
EQE (%)	5.53	5.27	4.91
Emission (nm)	455	455	455

recombination theory. A current conduction model with the occurrence of Langevin recombination in case of a single layer device with a polymer material was investigated by previous report [25]. This model was suggested based on the theory of conventional double-carrier semiconductor devices [25,26]. They assume that charge recombination and charge neutralization are of importance and recombination is bimolecular, i.e. that its rate is proportional to the product of the electron and hole concentrations. As a result, the current density in a double-carrier device can be considerably larger than in a single-carrier device. In the simple case without traps and a field independent mobility, the double-carrier current (plasma limit) is given by this equation [26];

$$J = \left(\frac{9\pi}{8}\right)^{\frac{1}{2}} \varepsilon_0 \varepsilon_r \left(\frac{2e\mu_p \mu_n (\mu_p + \mu_n)}{\varepsilon_0 \varepsilon_r B}\right)^{\frac{1}{2}} \frac{V^2}{L^3}$$

with B the bimolecular recombination constant. In order to quantitatively estimate the effect of our high current conduction, current conduction values of Device G and H were calculated with this equation because it is quite similar to our device concept and compared with real experimental results. For the calculation, our measured μ_p and μ_n values of 2.2×10^{-4} cm^2/Vs (NPB), 6.4×10^{-5} cm^2/Vs (2-TNATA), and 3.3×10^{-2} cm^2/Vs (HATCN) were used. For the L value, the general capture radius (r_c) of charge recombination in the organic materials was used as 18.5 nm. We assume that each 18.5 nm thickness of two interfaces in Device G and H gives us only this double carrier current behavior and remained 63 nm layer only gives us SCLC current values. For the B value, the reported values of 3.4×10^{-12} cm^3/s was used [27]. Table 2 shows our calculation result and experimental data. Calculated total current conduction values compared with single carrier devices are considerably increased due to these charge recombination interfaces. Even though experimental data are somewhat lower than calculation values, the order of magnitude for current enhancement is quite similar in both cases. Current enhancement by charge recombination interfaces in Device G and H is well understood by this double-carrier current equation. The mobility increases by insertion charge recombination interfaces also could be understood since mobility values are directly extracted by SCLC values. Our measured mobility values are obtained by assuming that our devices are

Table 2
Calculated current densities by a double-carrier current equation and experimental results in device G and H.

Voltage (V)	Device G		Device H	
	Experimental current density (A/cm^2)	Calculated current density (A/cm^2)	Experimental current density (A/cm^2)	Calculated current density (A/cm^2)
0.7	25.66	34.53	14.76	22.27
2.0	200.29	299.99	113.10	175.55
4.0	777.86	1076.80	435.13	676.97

single carrier devices. Therefore, carrier mobility increases of several orders of magnitude could be observed by insertion charge recombination interfaces. The effect of this mobility increase is very useful in organic semiconductor devices because current transportation behavior with non-radiative p-n-p interfaces is the same as single carrier devices and it can provide a new way to increase carrier mobility without new materials.

4. Conclusion

In summary, we have demonstrated enhanced current conduction with high mobility by multiple p-n-p junction structures in several organic devices. Voltage reduction in fluorescent blue OLEDs has been demonstrated by Langevin recombination theory. Multiple intrinsic p-n-p junctions can provide non-radiative coulombic interaction and thus carrier transportation is improved significantly. This multiple charge generation and recombination concept proposed in this study is capable of reducing the power consumption and rapid switching in various organic devices.

Acknowledgement

This work was supported by the Korea Science and Engineering Foundation (KOSEF) Grant funded by the Korea government (MEST).

References

[1] Y. Liang, G. Dong, Y. Hu, L. Wang, Y. Qiu, Appl. Phys. Lett. 86 (2005) 132101.
[2] D. Kumaki, T. Umeda, S. Tokito, Appl. Phys. Lett. 92 (2008) 013301.
[3] S. Duhm, H. Glowatzki, J.P. Rabe, N. Koch, R.L. Johnson, Appl. Phys. Lett. 90 (2007) 122113.
[4] Y. Gao, H. Ding, H. Wang, D. Yan, Appl. Phys. Lett. 91 (2007) 142112.
[5] I.H. Hong, M.W. Lee, Y.M. Koo, H. Jeong, T.S. Kim, O.K. Song, Appl. Phys. Lett. 87 (2005) 063502.
[6] Y. Kim, J.W. Kim, Y. Park, Appl. Phys. Lett. 94 (2009) 063305.
[7] T. Matsushima, Y. Kinoshita, H. Murata, Appl. Phys. Lett. 91 (2007) 253504.
[8] J. Meyer, S. Hamwi, T. Bülow, H.H. Johannes, T. Riedl, W. Kowalsky, Appl. Phys. Lett. 91 (2007) 113506.
[9] S.M. Park, Y.H. Kim, Y. Yi, H.Y. Oh, J.W. Kim, Appl. Phys. Lett. 97 (2010) 063308.
[10] L.S. Liao, W.K. Slusarek, T.K. Hatwar, M.L. Ricks, D.L. Comfort, Adv. Mater. 20 (2008) 324.
[11] H. Kanno, Y. Hamada, K. Nishimura, K. Okumoto, N. Saito, H. Ishida, H. Takakashi, K. Shibata, K. Mameno, Jpn. J. Appl. Phys. 45 (2006) 9219.
[12] D.J. Gundlach, J.E. Royer, S.K. Park, S. Subranaian, O.D. Jurchescu, B.H. Hamadani, A.J. Moad, R.J. Kline, L.C. Teague, O. Kirillov, C.A. Richter, J.G. Kushmerick, L.J. Richter, S.R. Parkin, T.N. Jackson, J.E. Anthony, Nature 7 (2008) 216.
[13] J.P. Hong, A.Y. Park, S. Lee, J. Kang, N. Shin, D.Y. Yoon, Appl. Phys. Lett. 92 (2008) 143311.
[14] L.C. Teague, B.H. Hamadani, O.D. Jurchescu, S. Subramanian, J.E. Anthony, T.N. Jackson, C.A. Richter, D.J. Gundlach, J.G. Kushmerik, Adv. Mater. 20 (2008) 4513.
[15] N.S. Stutzmann, E. Smits, H. Wondergem, C. Tanase, P. Blom, P. Smith, D.D. Leeuw, Nat. Mater. 4 (2005) 601.
[16] S.W. Park, J.M. Hwang, J.M. Choi, D.K. Hwang, M.S. Oh, J.H. Kim, S.G. Im, Appl. Phys. Lett. 90 (2007) 153512.
[17] Y. Wu, Y. Li, S. Gardner, B.S. Ong, J. Am. Chem. Soc. 127 (2005) 614.
[18] J. Locklina, M.E. Robertsa, Stefan C.B. Mannsfeld, Z. Baoa, Polym. Rev. 46 (2006) 79.
[19] I. Mcculloch, M. Heeney, C. Bailey, K. Genevicius, I. Macdonald, M. Shkunov, D. Sparrowe, S. Tierney, R. Wagner, W. Zhang, M.L. Chabinyc, R.J. Kline, M.D. Mcgehee, M.F. Toney, Nature 5 (2006) 328.
[20] M. Pope, C.E. Swenberg, Electronic Processes in Organic Crystals, Oxford University press, New York, USA, 1982.
[21] K.S. Swenberg, S.O. Jeon, J.Y. Lee, Thin Solid Films 517 (2009) 6109.
[22] M.A. Khan, W. Xu, K. Haq, Y. Bai, X.Y. Jiang, Z.L. Zhang, W.Q. Zhu, J. Appl. Phys. 103 (2008) 014509.
[23] S.C. Tse, K.C. Kwok, S.K. So, Appl. Phys. Lett. 89 (2006) 262102.
[24] M.H. Ho, Y.S. Wu, S.W. Wen, M.T. Lee, T.M. Chen, C.H. Chen, K.C. Kwok, S.K. So, K.T. Yeung, Y.K. Cheng, Z.Q. Gao, Appl. Phys. Lett. 89 (2006) 252903.
[25] P.W.M. Blom, M.C.J.M. Vissenberg, Mater. Sci. Eng. 27 (2000) 53.
[26] M.A. Lampert, P. Mark, Current Injection in Solids, Academic Press, New York, 1970.
[27] M.P. Eng, P.R.F. Barnes, James R. Durrant, J. Phys. Chem. Lett. 1 (2010) 3096.